JOURNAL OF Materials CHEMISTRY

Unusual electrocatalytic behavior of ferrocene bound fullerene cluster films

Said Barazzouk,† Surat Hotchandani† and Prashant V. Kamat*

Notre Dame Radiation Laboratory, Notre Dame, Indiana 46556-0579, USA.
E-mail: pkamat@nd.edu

Received 31st October 2001, Accepted 9th January 2002
First published as an Advance Article on the web 26 February 2002

Fullerene clusters containing a redox couple (ferrocene) have been assembled as nanostructured films on conducting glass and carbon electrodes using an electrophoretic approach. These films show irreversibility in the reduction waves when the electrochemical scan is limited to cathodic cycles (potential range of 0 to −0.8 V *versus* SCE). However, the reversibility in the cyclic voltammograms can be restored by extending the scans to the anodic region (+0.75 to −0.8 V *versus* SCE). The ferrocene couple reoxidizes the stabilized C_{60} anion–tetrabutylammonium complex in the cluster assembly during the oxidation cycle. We present here a simple approach of incorporating a redox active species for improving the electrochemical activity of fullerene films. The electrochemical measurements that illustrate the electrocatalytic property of C_{60} cluster films are described.

Introduction

To date, several approaches have been considered to develop electroactive and photoactive films of fullerene derivatives. These deposition techniques which include solvent evaporation,[1–4] molecular beam epitaxy,[5] Langmuir–Blodgett films,[6–8] self assembled monolayer assembly,[9–12] layer-by-layer assembly,[13] and electrophoresis[14] mainly produce polymorphous films. A high degree of molecular order has been achieved with the films formed on a pyrolytic graphite (HOPG).[15] Polymer films have also been used as hosts to develop electrochemically active fullerene films.[16,17] Both fullerene doped polymer films[18–21] and fullerene cluster films[14,22,23] have important applications in developing photovoltaic cells. Thin films of C_{60} and C_{60}–aniline dyads can also be conveniently cast on an electrode surface using an electrophoretic method from cluster solution.[14,22,23]

It is interesting to note that the C_{60} films constitute a new class of *carbon* electrodes with properties that differ from graphite and diamond electrodes. These films are quite stable to oxidative potentials and hence are suitable to carry out oxidation processes. Moreover, C_{60} cluster films cast by electrodeposition methods on nanostructured SnO_2 films are photoelectrochemically active and are capable of producing photocurrents up to 0.2 mA cm^{-2}.[22,23] However, fullerene films cast on an electrode surface show unusual electrochemical dependence on the method of preparation and the electrolyte medium.[24] The one- and two-electron-reduced forms of C_{60} undergo complexation with the cation (for example, tetrabutylammonium ion in acetonitrile medium) and exhibit a hysteresis in the cyclic voltammograms. The variation in the film morphology also affects the rate of ion transport within the C_{60} film.[25]

Recently, we have demonstrated the feasibility of forming spherical assemblies of C_{60} and electron donors (ferrocene, amines, phenothiazine) as optically transparent clusters in mixed solvents.[26] The microheterogeneous environment of fullerene clusters facilitates trapping of electron donor molecules from solution. Efficient quenching of the excited states and formation of long lived electron transfer products, following the photoexcitation of the fullerene cluster–electron donor assemblies were monitored through laser flash photolysis experiments.[26,27] Intramolecular electron transfer in fullerene/ferrocene based donor–bridge–acceptor dyads have also been studied.[28] However, electrochemical studies that elucidate the interaction between fullerene and an electron donor system are rather limited.[24] Of particular interest is the role of fullerene anions, which upon stabilization with protons[29] or alkali metal ions[30,31] dictate the electrochemical activity of the fullerene films. We have now incorporated a redox couple, *viz.*, ferrocene in C_{60} clusters, and assembled these clusters as thin films on electrode surfaces. The ability of a redox couple in modulating the electrochemical properties of fullerene films is demonstrated. The results that show the electrocatalytic behavior of ferrocene incorporated fullerene film are presented here.

Experimental

A suspension of C_{60} clusters (99.99% purity C_{60}, obtained from SES Research) was prepared by injecting toluene solutions of C_{60} (500 μl, 1 mM) into a pool of 4.5 ml acetonitrile containing ~ 0.12 mM ferrocene (Fc). The final solvent ratio of mixed solvent was 9 : 1 (v/v) acetonitrile : toluene. A rapid change to yellow-brown coloration confirms the formation of fullerene clusters in solution. We refer to these clusters as Fc@ $(C_{60})_n$.

A known amount (~2 mL) of Fc@ $(C_{60})_n$ cluster suspension (0.1 mM of C_{60} and ~12 mM of Fc) was transferred to a 1 cm cuvette in which two optically transparent electrodes (OTE) were kept at a distance of ~6 mm using a Teflon spacer. A dc voltage (100–200 V) was applied using a Fluke 415 high voltage dc power supply (see reference 22 for cell design). Within 30–60 seconds the solution turned colorless as all the Fc@$(C_{60})_n$ clusters were deposited as a brown film on the electrode connected to the positive terminal of the source. The electrode was thoroughly washed with acetonitrile. Cyclic voltammetry measurements of the cluster solution before and after depositing film on the OTE indicated a loss of 30–40% of ferrocene. This loss accounts for the net incorporation of ferrocene into the cluster film. A similar method was employed

†*Permanent address*: Groupe de Recherche en Énergie et Information Biomoléculaires, Université du Québec à Trois-Rivières, Trois Rivières, Québec, Canada G9A 5H7.

to cast films of C_{60} and Fc@$(C_{60})_n$ clusters on a glassy carbon electrode.

The UV–visible spectra were recorded on a Shimadzu 3101PC spectrophotometer. Cyclic voltammograms were recorded with a BAS 100B Electrochemical analyzer. Unless otherwise specified the electrochemical experiments were conducted using $(C_{60})_n$ or Fc@$(C_{60})_n$ working electrode, Pt counter electrode, saturated calomel reference electrode (SCE) and acetonitrile solution containing 0.1 M tetrabutylammonium perchlorate (TBAP) as the electrolyte. The AFM images were recorded in tapping mode using a Nanoscope III (Digital Instruments).

Results and discussion

Fullerenes, C_{60} and C_{70}, and their derivatives form optically transparent microscopic clusters (diameter 100–300 nm) in mixed solvents at room temperature.[32–35] Clustering of fullerene molecules is mainly associated with the strong three-dimensional hydrophobic interactions between fullerene units. Details of the conditions for the formation of the aggregate clusters of fullerenes as well as their spectroscopic properties[32,36] and size distribution studies[32] are well documented. In a recent study, formation of spherical bilayered vesicles in a polar–nonpolar solvent mixture has been demonstrated using functionalized fullerene molecules, $(C_6H_5)_5C_{60}K$.[37] These spherical cluster aggregates behave as rigid hydrophobic nanoballs with dominant geometric constraints.

The C_{60} clusters can become charged under the influence of a dc electric field and get deposited on the positive electrode. The desired thickness and morphology of the film can be achieved by controlling the deposition voltage and the fullerene concentration in toluene solution. The ability to assemble the fullerene clusters as 3-dimensional arrays opens up new avenues to design high surface area electrode materials that are potentially useful for developing chemical sensors and light energy conversion devices. A schematic illustration of the electrodeposition process is illustrated in Fig. 1.

Absorption characteristics of the fullerene clusters

The absorption spectra of C_{60} and Fc@$(C_{60})_n$ films on OTE are shown in Fig. 2. The solution spectrum of C_{60} in toluene is also shown for comparison. As compared to the solution spectrum of pristine C_{60}, the cluster spectrum is rather broad. Increase in the molar absorptivity of fullerene clusters is a characteristic of intermolecular interactions in both cluster suspensions and in films. The absorption spectrum of clusters in the 400–550 nm region exhibits a featureless, broad absorption. Intermolecular interaction between the fullerene moieties contribute to the increased absorptivity.[27,34]

The presence of ferrocene in acetonitrile during the clustering process allows its incorporation into the C_{60} clusters. Cyclic voltammetry experiments carried out with cluster solutions show ~40% loss of ferrocene during the electrophoretic deposition process. Photoinduced electron transfer processes carried out with C_{60}–donor clusters also have confirmed incorporation of ferrocene moieties in fullerene clusters.[26] Upon electrodeposition, fullerene clusters containing ferrocene groups are assembled as 3-dimensional network arrays on the electrode surface. The films of Fc@$(C_{60})_n$ show a prominent absorption band around 450 nm (Fig. 2, curve c). This increased absorption in the visible arises from ferrocene, which has a strong absorption in the 370–520 nm with a broad maximum around 450 nm. This increased absorption of Fc@$(C_{60})_n$ film compared to neat $(C_{60})_n$ film in the visible region further confirms the incorporation of ferrocene in the C_{60} cluster assembly. It should be noted that the ferrocene is strongly held in the film and does not leach out even after repeated washing or immersing in acetonitrile.

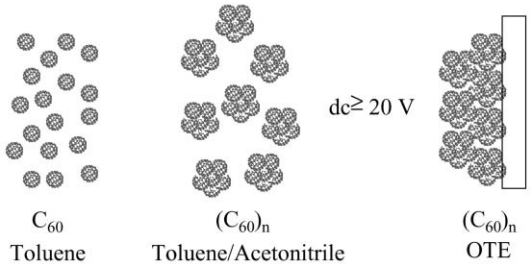

Fig. 1 Assembling fullerene clusters as nanostructured films on an electrode surface.

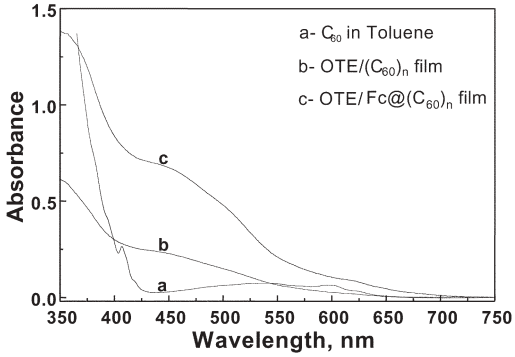

Fig. 2 Absorption spectra of (a) C_{60} in toluene; (b) $(C_{60})_n$ cluster film; and (c) Fc@$(C_{60})_n$ cluster film.

Atomic force microscopy

In a previous study[14] we have shown that C_{60} cluster film cast on a conducting glass electrode shows a 3-D assembly of spherical clusters of 100–150 nm diameter. By assembling the fullerene clusters in an orderly fashion, we were able to develop high surface area electrodes with excellent photoelectrochemical response.[22] In the present study we probed the morphology of the electrophoretically assembled Fc@$(C_{60})_n$ cluster film using atomic force microscopy (AFM). Fig. 3 shows the AFM images of a Fc@$(C_{60})_n$ cluster film deposited on OTE at a deposition voltage of 50 V. The AFM images show a 3-dimensional assembly of Fc@$(C_{60})_n$ clusters on the electrode surface. The electrophoretically deposited cluster film is highly porous and consists of Fc@$(C_{60})_n$ clusters that are assembled in a fairly orderly fashion. The original cluster diameter of 50–100 nm in suspension is well retained during electrophoretic deposition process. However, additional aggregation of these individual clusters during film formation is evident from Fig. 3. Several Fc@$(C_{60})_n$ clusters seem to coalesce and form larger aggregates of spherical shape (diameter 300–500 nm). The AFM image scanned at higher resolution shows the ordering of Fc@$(C_{60})_n$ clusters as nanoballs, thus giving a fine nanostructure to the fullerene film. Note that each of these aggregated nanoballs consists of 50–100 nm diameter C_{60} clusters of varying shapes.

Electrochemistry of fullerene cluster films at conducting glass electrode

Several studies in the past have reported the redox behavior of fullerene films cast on electrode surfaces.[1,16,24,25,29,38] The redox activity of these films depends upon the method of deposition and the medium in which the C_{60} film is exposed. For example, the first and second electron reduction waves of C_{60} films are merged to yield a broad reduction wave.[25] It was also pointed out that the swelling of the C_{60} film plays an important role in controlling the redox activity of the film. The

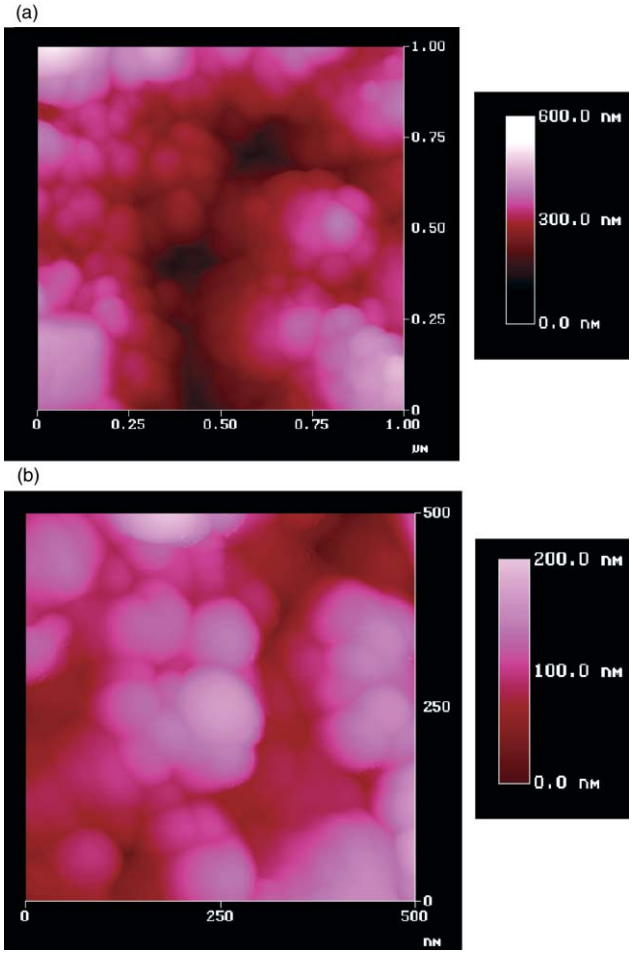

Fig. 3 AFM images of $Fc@(C_{60})_n$ cluster film cast on a conducting glass electrode using electrophoretic deposition methods. The images were recorded using tapping mode, at two different resolutions.

swelling of the film allows penetration of cations and redox active species such as ferrocene from solution. In another independent study, increased conductivity of the reduced film was confirmed in the presence of alkali metal cations.[30,31] Because of this unusual redox chemistry of C_{60} films, we carefully examined the cyclic voltammograms of $Fc@(C_{60})_n$ films.

Fig. 4 shows the cyclic voltammograms of $Fc@(C_{60})_n$ film deposited on a conducting glass electrode. In Fig. 4A, the scans were limited to the potential range of 0 to −0.7 V *vs.* SCE. In this potential range we expect to observe one-electron reduction of C_{60}. This reduction is quite evident in the first scan with a prominent peak around −0.55 V. Upon reversal of the scan we could not observe any peaks corresponding to reoxidation of C_{60} anion. Further scans showed less prominent reduction peaks with a decrease in the magnitude of current. The irreversibility became more prominent when we extended the potential range to −1.2 V *vs.* SCE and carried out higher reductions. Although C_{60} exhibits well separated reversible reduction peaks (up to six 1-electron reductions) when dissolved in solution, the reduction profiles of C_{60} films have remained a perplexing issue.[24] The one electron reduction shown in Fig. 4A further ascertains the fact that the reversibility of C_{60} reduction is greatly suppressed when pristine C_{60} deposited as cluster films.

Fig. 4B shows the cyclic voltammograms of $Fc@(C_{60})_n$ cluster film scanned under a wider potential range of +0.8 to −0.7 V *versus* SCE. Two distinct features were seen in these scans. First, the cyclic voltammograms became reproducible when scanned repeatedly in the potential range of +0.8 to −0.7 V *versus* SCE. The reduction peak around −0.55 V

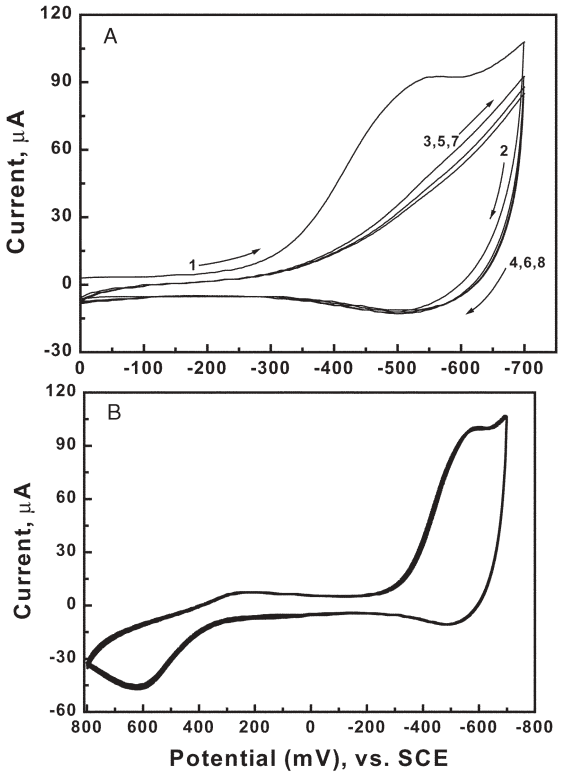

Fig. 4 Cyclic voltammogram of (A) $(C_{60})_n$ cluster film and (B) $Fc@(C_{60})_n$ cluster films deposited on a conducting glass electrode (electrolyte: 0.1 M TBAP in acetonitrile, scan rate 50 mV s^{-1}).

remains quite broad, similar to the one observed in the first scan of Fig. 4A indicating that the overall reduction of C_{60} in the film is not influenced by the presence of ferrocene. Secondly, the cyclic voltammograms exhibited an oxidation peak at +0.65 V *versus* SCE corresponding to the ferrocene oxidation. The interesting observation stems from the enhanced anodic peak corresponding to the oxidation of Fc^0/Fc^+ at +0.65 V. Although the anodic and cathodic peak heights were mismatched in terms of peak current, the reversibility of the cyclic voltammogram was well maintained in repetitive scans. In order to understand the electrochemical behavior of $Fc@(C_{60})_n$ films, we extended our studies using glassy carbon electrodes.

Reversibility of the Fc^0/Fc^+ couple in the $Fc@(C_{60})_n$ film

Fig. 5A shows the cyclic voltammograms of $Fc@(C_{60})_n$ clusters film deposited on a glassy carbon electrode recorded at different scan rates in the potential range where we expect to see the oxidation of ferrocene. The cyclic voltammograms show matching oxidation (430 mV) and reduction (360 mV) peaks as one would expect from a Fc/Fc^+ couple. Note that the potential scan for these measurements is limited to a range of +0.75 −0 V *vs.* SCE. There is no involvement of the redox behavior of C_{60} in this potential range. Thus, we can conclude that the ferrocene incorporated in the C_{60} film is electroactive and undergoes reversible oxidation at 395 mV *vs.* SCE. The difference in peak potentials is likely to arise from the diffusivity of the electroactive species within the film and/or resistance of the C_{60} film. Further confirmation for the entrapment of ferrocene in the C_{60} cluster film is obtained from the analysis of peak currents at different scan rates. With increasing scan rates both cathodic and anodic peak currents increase without distortion of the peak shapes (Fig. 5A). The linear increase in anodic and cathodic peak current *versus* the scan rate (Fig. 5B) confirms that the observed cyclic voltammogram is a surface wave. This observation further confirms that the ferrocene molecules are retained in the C_{60} cluster film

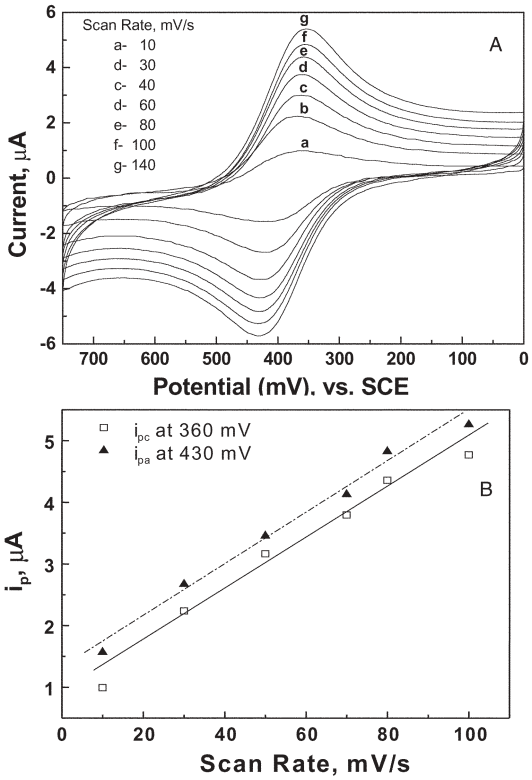

Fig. 5 A. Cyclic voltammogram of Fc@$(C_{60})_n$ cluster films deposited on a glassy carbon electrode at different scan rates (electrolyte: 0.1 M TBAP in acetonitrile) B. Dependence of anodic (i_{pa} monitored at 430 mV) and cathodic (i_{pc} monitored at 360 mV) peak currents *versus* scan rate. The cyclic voltammogram scans were limited to ferrocene oxidation only (experimental conditions were same as in Fig. 5A).

even after repeated cycling in acetonitrile solutions containing TBAP.

Electrocatalysis using Fc@$(C_{60})_n$ films

We further evaluated the electrochemical behavior of ferrocene@$(C_{60})_n$ films with repeated scans in the potential range of +0.7 to −0.8 V *vs.* SCE. Fig. 6 shows the successive runs of this experiment. In the initial anodic scan (scan #1 & 2) we observe a reversible oxidation peak corresponding to the one-electron oxidation of ferrocene. The reversible oxidation peak is similar to the one observed in Fig. 5A. The C_{60} cluster films that were deposited without incorporating ferrocene do not exhibit any oxidation peaks (inset in Fig. 6), thereby confirming the

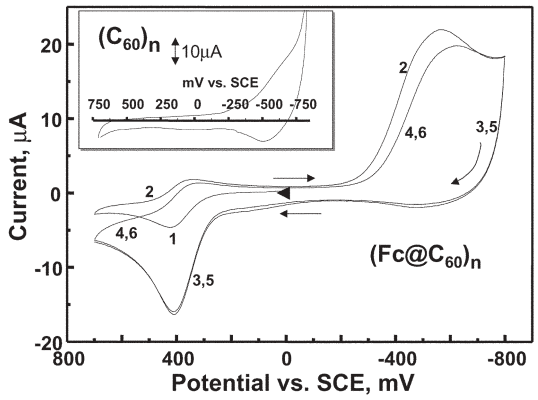

Fig. 6 Cyclic voltammogram of Fc@$(C_{60})_n$ cluster film deposited on a glassy carbon electrode (electrolyte: 0.1 M TBAP in acetonitrile, scan rate 20 mV s^{-1}) The arrows indicate the direction of scan. Inset shows the cyclic voltammogram of C_{60} cluster film deposited in the absence of ferrocene.

stability of C_{60} to electrochemical oxidation at potentials below 1 V. At negative potentials we observe a broad cathodic peak around −590 mV, which corresponds to the reduction of C_{60}. The two scans (#1 & 2) in Fig. 6 exhibit a normal electrochemical behavior that one would anticipate from the cyclic voltammograms of two electroactive species, *viz.* Fc^0/Fc^+ and C_{60}/C_{60}^-. Upon reversal of the scan following the reduction of C_{60} (scan #3) we observe a different behavior. A significant enhancement is seen for the oxidation peak at potential corresponding to ferrocene oxidation. This enhanced oxidation peak represents increased oxidation events that involve Fc^0. This behavior is similar to that observed in Fig. 4B and confirms the reproducibility of the electrochemical behavior of Fc@$(C_{60})_n$ at both glassy carbon and conducting glass electrodes.

The unusual electrochemical behavior observed in the anodic scan can be attributed to the catalytic process mediated by C_{60} anions in the cluster films (reactions 1–4).

$$\text{At } -0.6 \text{ V: } (C_{60})_n \rightarrow (C_{60})_n^- — TBA^+ \rightarrow \{(C_{60})_n^- – TBA^+\} \quad (1)$$

$$\text{At } +0.43 \text{ V: } Fc^0 \rightarrow Fc^+ \quad (2)$$

$$\text{Catalytic reaction: } Fc^+ + \{(C_{60})_n^- – TBA^+\} \rightarrow Fc^0 + (C_{60})_n + TBA^+ \quad (3)$$

$$\text{At } +0.36 \text{ V: } Fc^+ \rightarrow Fc^0 \quad (4)$$

Once the C_{60} in the cluster film undergoes reduction (reaction 1), the anion gets stabilized in the cluster film. As discussed in an earlier work,[25] the complexation between the C_{60} anion and tetrabutylammonium cation (TBA^+) is responsible for the stabilization of reduced species in the cluster film. Szucs *et al.*[30,31] have demonstrated that the cation stabilized reduced films of C_{60} remain stable even when exposed to air. As evident from the cyclic voltammograms in Fig. 6, the stabilized $\{(C_{60})_n^- – TBA^+\}$ species are not directly accessible for reoxidation at the electrode surface. The stabilized $\{(C_{60})_n^- – TBA^+\}$ species is retained in the film undisturbed until the electrochemical scan reaches a potential around +300 mV. At this potential, the Fc^0 in the film starts to be oxidized (reaction 2). As soon as ferrocene is oxidized, it extracts the electron from $\{(C_{60})_n^- – TBA^+\}$ and regenerates the ferrocene in the cluster film (reaction 3).

Continuous oxidation and regeneration events (reactions 2 and 3) at this ferrocene oxidation potential (E^0 = 395 mV) render the anodic peak current to rise sharply. Once all the $\{(C_{60})_n^- – TBA^+\}$ in the film is consumed, a saturation in anodic current is reached (E_{pa} = 430 mV). At this point all the ferrocene in the film gets converted into its oxidized form. In the reverse scan (scan #4) we observe the usual reduction wave of Fc^+ (reaction 4). Note that the reduction peak currents (E_{pc} = 360 mV) in the reverse scans #2 and 4 are similar. This observation suggests that the net amount of oxidized ferrocene in the C_{60} cluster film remains unchanged. Continuous scanning in the range of +0.75 to −0.8 V *versus* SCE produces reproducible traces with no loss in the electrochemical activity of C_{60} and ferrocene. By adding a reversible redox couple in the C_{60} cluster film we have succeeded in maintaining a complete electrochemical reversibility of the film. The electrochemical events of ferrocene incorporated C_{60} cluster film are illustrated in Fig. 7.

It should be noted that the enhancement in the anodic peak current of ferrocene oxidation is observed only when the electrochemical scan is preceded by the reduction of C_{60}. Since the total amount of ferrocene involved in the oxidation process remains constant, the enhancement seen in the oxidation peak current should be attributed to the catalytic oxidation mediated by the C_{60} anion–TBA^+ complex. In the past, such electrocatalytic reactions have been studied in detail with $Ru(bpy)_3^{2+}$

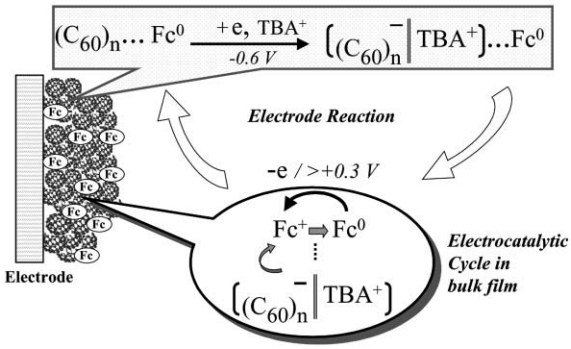

Fig. 7 Mechanism of electrochemical events at a Fc@$(C_{60})_n$ cluster film electrode.

incorporated Nafion,[39,40] and croconate dye and ferrocyanide incorporated poly(4-vinylpyridine) films.[41–43] The electroactive species in the polymer film were shown to mediate the oxidation of the bulk species present in solution. An important aspect of the electrocatalytic reaction is to improve the sensitivity of electrochemical detection by increasing the oxidation–reduction turnover events at the detection potential. For example, in the experiment discussed above a reduced C_{60} film can yield more than 5 times higher anodic current than the unreduced C_{60} film during the oxidation of ferrocene.

Conclusions

Ferrocene incorporated fullerene clusters have been assembled as thin films on conducting glass and glassy carbon electrodes. A simple approach of incorporating electrochemically active species in the fullerene film can significantly improve the electrochemical activity of the fullerene film. These electroactive C_{60} cluster films exhibit electrocatalytic behavior by modulating the oxidation of the ferrocene redox couple. The ability of C_{60} film to participate in an electrocatalytic reaction should prove useful in the detection and analysis of solutes at low concentration levels. Such an interesting property opens up new avenues for developing fullerene based electrochemical sensors.

Acknowledgement

We would like to acknowledge the support of the Office of Basic Energy Science of the Department of Energy to conduct the research described here. This is contribution No NDRL 4346 from the Notre Dame Radiation Laboratory. SB and SH acknowledge the support of Natural Sciences and Engineering Research Council of Canada.

References

1 B. Miller, J. M. Rosamilia, G. Dabbagh, R. Tycko, R. C. Haddon, A. J. Muller, W. Wilson, D. W. Murphy and A. F. Hebard, *J. Am. Chem. Soc.*, 1991, **113**, 6291.
2 S. Licht, O. Khaselev, P. A. Ramakrishnan, D. Faiman, E. A. Katz, A. Shames and S. Goren, *Solar Energy Mater. Solar Cells*, 1998, **51**, 9.
3 J. J. Davis, H. A. O. Hill, A. Kurz, A. D. Leighton and A. Y. Safronov, *J. Electroanal. Chem.*, 1997, **429**, 7.
4 M. Csiszar, A. Szucs, M. Tolgyesi, J. B. Nagy and M. Novak, *J. Electroanal. Chem.*, 1998, **441**, 287.
5 C. Kvarnstrom, H. Neugebauer, G. Matt, H. Sitter and N. S. Sariciftci, *Synth. Met.*, 1999, **103**, 2430.
6 C. P. Luo, C. H. Huang, L. B. Gan, D. J. Zhou, W. S. Xia, Q. K. Zhuang, Y. L. Zhao and Y. Y. Huang, *J. Phys. Chem. B*, 1996, **100**, 16685.
7 W. Zhang, Y. Shi, L. Gan, C. Huang, H. Luo, D. Wu and N. Li, *J. Phys. Chem. B*, 1999, **103**, 675.
8 D. M. Guldi, M. Maggini, S. Mondini, F. Guerin and J. H. Fendler, *Langmuir*, 2000, **16**, 1311.
9 T. Akiyama, H. Imahori, A. Ajawakom and Y. Sakata, *Chem. Lett.*, 1996, 907.
10 H. Imahori, T. Azuma, A. Ajavakom, H. Norieda, H. Yamada and Y. Sakata, *J. Phys. Chem. B*, 1999, **103**, 7233.
11 O. Enger, F. Nuesch, M. Fibbioli, L. Echegoyen, E. Pretsch and F. Diederich, *J. Mater. Chem.*, 2000, **10**, 2231.
12 P. K. Sudeep, B. I. Ipe, K. George Thomas, M. V. George, S. Barazzouk, S. Hotchandani and P. V. Kamat, *Nano Lett.*, 2002, **2**, 29.
13 C. P. Luo, D. M. Guldi, M. Maggini, E. Menna, S. Mondini, N. A. Kotov and M. Prato, *Angew. Chem., Int. Ed.*, 2000, **39**, 3905.
14 P. V. Kamat, S. Barazzouk and S. Hotchandani, *Adv. Mater.*, 2001, **13**, 1614.
15 P. Janda, T. Krieg and L. Dunsch, *Adv. Mater.*, 1998, **10**, 1434.
16 A. Deronzier and J.-C. Moutet, *J. Am. Chem. Soc.*, 1994, **116**, 5019.
17 S. Bouchtalla, A. Deronzier, J. M. Janot, J. C. Moutet and P. Seta, *Synth. Met.*, 1996, **82**, 129.
18 G. Yu, J. Gao, J. C. Hummelen, F. Wudl and A. J. Heeger, *Science*, 1995, **270**, 1789.
19 G. Yu, J. Gao, J. C. Hummelen, F. Wudl and A. J. Heeger, *Science*, 1995, **270**, 1789.
20 J.-F. Nierengarten, J.-F. Eckert, J.-F. Nicoud, L. Ouali, V. Krasnikov and G. Hadziioannou, *Chem. Commun.*, 1999, 617.
21 E. Peeters, P. A. van Hal, J. Knol, C. J. Brabec, N. S. Sariciftci, J. C. Hummelen, A. René and R. A. J. Janssen, *J. Phys. Chem. B*, 2000, **104**, 10174.
22 P. V. Kamat, S. Barazzouk, K. George Thomas and S. Hotchandani, *J. Phys. Chem. B*, 2000, **104**, 4014.
23 P. V. Kamat, S. Barazzouk, S. Hotchandani and K. George Thomas, *Chem. Eur. J.*, 2000, **6**, 3914.
24 J. Chlistunoff, D. Cliffel and A. J. Bard, *Thin Solid Films*, 1995, **257**, 166.
25 J. F. Carlisle, C. A. Wijayawardhana, T. A. Evans, P. R. Melaragno and I. B. Alin-Pyzik, *J. Phys. Chem.*, 1996, **100**, 15532.
26 V. Biju, S. Barazzouk, K. George Thomas, M. V. George and P. V. Kamat, *Langmuir*, 2001, **17**, 2930.
27 K. George Thomas, V. Biju, M. V. George, D. M. Guldi and P. V. Kamat, *J. Phys. Chem. B*, 1999, **103**, 8864.
28 D. M. Guldi, M. Maggini, G. Scorrano and M. Prato, *J. Am. Chem. Soc.*, 1997, **119**, 974.
29 D. E. Cliffel and A. J. Bard, *J. Phys. Chem.*, 1994, **98**, 8140.
30 A. Szucs, A. Loix, J. B. Nagy and L. Lamberts, *J. Electroanal. Chem.*, 1995, **397**, 191.
31 A. Szucs, A. Loix, J. B. Nagy and L. Lamberts, *J. Electroanal. Chem.*, 1996, **402**, 137.
32 Y.-P. Sun, B. Ma, C. E. Bunker and B. Liu, *J. Am. Chem. Soc.*, 1995, **117**, 12705.
33 A. Beeby, J. Eastoe and R. K. Heenan, *J. Chem. Soc., Chem. Commun.*, 1994, 173.
34 Y. M. Wang, P. V. Kamat and L. K. Patterson, *J. Phys. Chem.*, 1993, **97**, 8793.
35 S. Nath, H. Pal, D. K. Palit, A. V. Sapre and J. P. Mittal, *J. Phys. Chem. B*, 1998, **102**, 10158.
36 D. M. Guldi, H. Hungerbuehler and K. D. Asmus, *J. Phys. Chem.*, 1995, **99**, 13487.
37 S. Zhou, C. Burger, B. Chu, M. Sawamura, N. Nagahama, M. Toganoh, U. E. Hackler, H. Isobe and E. Nakamura, *Science*, 2001, **291**, 1944.
38 C. Jehoulet and A. J. Bard, *J. Am. Chem. Soc.*, 1994, **113**, 5456.
39 C. R. Martin, I. Rubinstein and A. J. Bard, *J. Am. Chem. Soc.*, 1982, **104**, 4817.
40 M. Krishnan, X. Zhang and A. J. Bard, *J. Am. Chem. Soc.*, 1984, **106**, 7371.
41 N. Oyama and F. C. Anson, *Anal. Chem.*, 1980, **52**, 1192.
42 P. V. Kamat and M. A. Fox, *J. Electroanal. Chem.*, 1983, **159**, 49.
43 P. V. Kamat, M. A. Fox and A. J. Fatiadi, *J. Am. Chem. Soc.*, 1984, **106**, 1191.